Aryl Fluoride Activation Through Palladium-Magnesium Bimetallic Cooperation: A Mechanistic and Computational Study

Chen Wu,[‡] Samuel P. McCollom,[‡] Zhipeng Zheng, Jiadi Zhang, Sheng-chun Sha, Minyan Li, Patrick J. Walsh,* Neil C. Tomson*

Roy and Diana Vagelos Laboratories, Department of Chemistry, University of Pennsylvania, 231 South 34th Street, Philadelphia, Pennsylvania 19104-6323, United States

Inorganic Chemistry, Organic Chemistry, Catalysis, Organometallics

ABSTRACT: Herein is described a mechanistic study of a palladium-catalyzed cross-coupling of aryl Grignard reagents to fluoroarenes that proceeds via a low-energy heterobimetallic oxidative addition pathway. Traditional oxidative additions of aryl chlorides to Pd complexes are known to be orders of magnitude faster than with aryl fluorides, and many palladium catalysts do not activate aryl fluorides at all. The experimental and computational studies outlined herein, however, support the view that at elevated Grignard: ArX ratios (i.e. 2.5:1) a Pd-Mg heterobimetallic mechanism predominates, leading to a remarkable decrease in the energy required for Ar–F bond activation. The heterobimetallic transition state for C–X bond cleavage is proposed to involve simultaneous Pd backbonding to the arene and Lewis acid activation of the halide by Mg to create a low-energy transition state for oxidative addition. The insights gained from this computational study led to the development of a new phosphine ligand design that was shown to be similarly competent for Ar–F bond activation.

1. Introduction

C–F bonds have garnered widespread attention as challenging and attractive targets for materials science, pharmaceuticals, and agrochemicals. At a bond strength of 126 kcal/mol, the C–F bond in fluorobenzene is among the strongest in organic chemistry, and as a result, it is considerably more difficult to cleave than the C–Cl bond in aryl chlorides (96 kcal/mol). Due in large part to this high bond strength, aryl fluorides are inert in the presence of most cross-coupling catalysts. Therefore, the development of methods for facile aryl fluoride activation can allow for selective, late-stage modifications following passage through a range of demanding synthetic transformations. ^{3, 6-9}

Many examples are known in which nickel is able to promote cross coupling with Ar–F-based electrophiles. ¹⁰⁻¹⁴ The nickel chemistry typically requires sterically demanding and electronrich ligands. The lower electronegativity of nickel relative to palladium engenders nickel catalysts with greater ability to oxidatively add strong bonds, including aryl fluorides. ¹⁰ Compared with nickel catalysts, however, palladium catalysts have been extensively studied across a variety of cross-coupling reactions. Towards this end we focused on Pd, as there are a wide variety of phosphine ligands geared toward Pd cross-coupling catalysis.

In comparison with nickel, ¹⁰ palladium-catalyzed cross-coupling chemistry with aryl fluorides is rare, and typically the aryl fluoride must be activated. ¹⁵⁻²¹ Modes of activation (Figure 1) include the η^6 -coordination of the aryl fluoride to transition metal complexes such as $Cr(CO)_3$, $^{18-19}$ the use of aryl fluorides with strongly electron withdrawing groups, $^{16,\ 21}$ and the use of directing groups to position the palladium in close proximity to the C–F bond. $^{17-18}$ Few examples exist of Pd-catalyzed cross-coupling of unactivated

aryl fluorides, which have been shown to couple with amines,²² organotin reagents,²² organoboron reagents,^{16, 22} terminal alkynes²³⁻²⁵ and Grignard reagents.²² In the sole example of cross-coupling aryl fluorides with Grignard reagents, Dankwardt described the use of Pd(dba)₂ (5 mol%)/ PCy₂Ph (7.5 mol%) with 3 equiv of ArMgCl at 80 °C for 60 h (Figure 1d).¹⁵ The coupling products were formed with GC yield of 21 to 65 % (6 substrates), limiting the potential utility of this process. In one example it was shown that microwave irradiation in THF at 150 °C led to 98% GC yield. In late 2019, Zhao and coworkers published a high yielding palladium catalyzed Sonogashira-type coupling reaction with aryl fluorides and terminal alkynes (Figure 1e). An unconventional palladium catalyst, prepared by addition of LiN(SiMe₃)₂ to Pd₂(dba)₃ was found to be active in this coupling reaction.²⁵

We have previously reported use of the Bronsted acidic NIXANTPHOS ligand, designed by van Leeuwen and coworkers, 26-27 for the coupling of diarylmethanes with aryl bromides and chlorides. 28-29 Under the basic reaction conditions needed to effect C-C bond formation, the NIXANTPHOS ligand's N-H was deprotonated ($pK_a = \sim 21$ in DMSO), generating an anionic ligand that binds potassium to both the nitrogen and the backbone of the ligand's aromatic π -system.²⁸-²⁹ This heterobimetallic catalyst was shown to oxidatively add unactivated aryl chlorides at room temperature, indicating a substantial decrease in activation energy compared to other palladium catalysts bearing bidentate ligands. 30-33 hypothesized that the exceptional reactivity of this system stems from the cooperativity between the main group metal and the palladium catalyst (Figure 2a). Support for this cooperativity via cation- π interactions has recently been shown through both the chemoselective functionalization of 2-benzylfuran³⁴ and the arylation of toluene.35-36

The use of heterobimetallic catalysts to activate strong bonds has been studied over the years. Noteworthy bimetallic transition states for C–X bond activation by Nakamura are shown in Figure 2b³⁷⁻³⁸ and c.³⁹⁻⁴⁰ Of particular note, this group developed a strategy to activate C–F bonds for nickel-catalyzed cross-couplings using a novel hydroxyphosphine ligand in which an alkoxy-bridged Ni–Mg heterobimetallic complex was proposed as key to Ar–F activation (Figure 2c).³⁹ This heterobimetallic catalyst system can activate aryl fluorides in good yields at 5 mol % loading.⁴¹ It would be advantageous to perform heterobimetallic aryl fluoride activation using ligands that are more readily available.

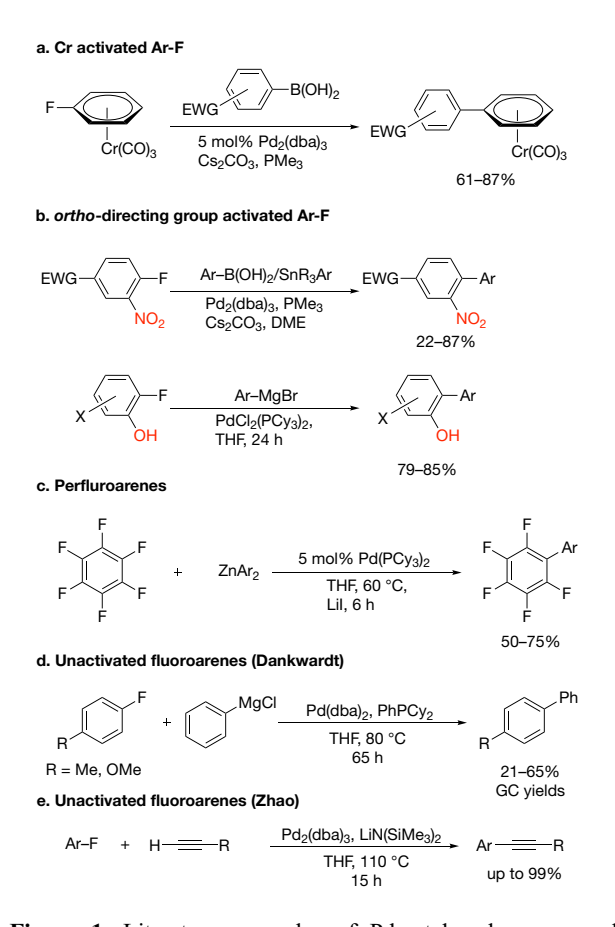


Figure 1. Literature examples of Pd-catalyzed cross-coupling reactions with aryl fluorides. Activation of the substrates by: **a.** coordination to a transition metal; **b.** use of directing groups; **c.** employing electron poor aryl fluorides. **d.** Cross-coupling of unactivated aryl fluorides with Grignard reagents by Dankwardt and coworkers; **e.** Coupling of aryl fluorides with a palladium catalyst by Zhao.

Building on this precedent with the use of the NIXANTPHOS-based catalyst, ²⁸⁻²⁹ we sought a class of ligands that would promote the cleavage of Ar–F bonds through a heterobimetallic activation processes. Although there are many Grignard reagents that are readily available or easily synthesized, ⁴²⁻⁴³ we chose to focus on the characteristics of the ligand that enabled activation of strong C–F bonds. A high-throughput experimentation screen of Pd-catalyzed

Kumada-Tamao-Corriu (KTC) cross-coupling reactions⁴⁴ with a variety of potential auxiliary ligands identified a class of phosphines that promote Ar–F bond activation under mild conditions and short reaction times. Following initial mechanistic studies, density functional theory (DFT) calculations were used to support the proposal that a Mg ion from the Grignard reagent is intimately involved in oxidative addition of the C–F bond. These findings point to a novel mechanism for KTC cross-coupling reactions that can occur under Grignard : electrophile ratios commonly used in cross-coupling reactions.

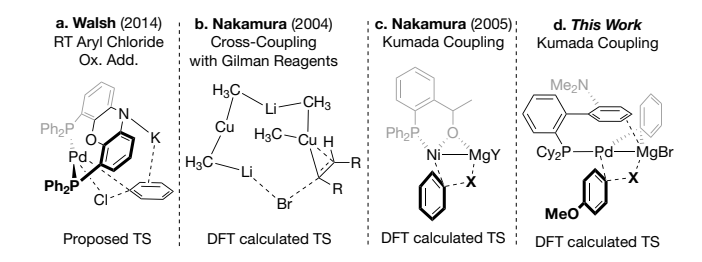


Figure 2. Key transition states involving heterobimetallic cooperativity. From left to right: **a.** Our prior work; **b.** Nakamura (2004); **c.** Nakamura (2005); **d.** this work.

2. Results and Discussion

2.1 Catalyst Identification and Optimization

The KTC cross-coupling of 4-fluorobiphenyl, **1a**, and 4-*tert*-butyl-phenyl magnesium bromide (**2a**) was used as a test reaction. A ligand screen was performed using high-throughput experimentation (10 μmol of Ar–F **1a**, 25 μmol of Grignard reagent **2a**, 10 mol % of Pd(OAc)₂, 20 mol % for monodentate phosphines, 10 mol % for bidentate ligands, 80 °C, in THF for 16 h). Of the 48 phosphine ligands, the most promising were cataCXium PCy, DavePhos and CyJohnPhos, all of which share a similar structural motif of two cyclohexyl groups and one biphenyl-type group (Table 1). Notably, without added phosphine ligand, Pd(OAc)₂ alone provided an assay yield of 22 % under these conditions, and the exclusion of Pd(OAc)₂ from the reaction mixture gave 0 % yield.

These three ligands were then optimized on laboratory scale (0.1 mmol) with 5 mol % loading of Pd(OAc)₂ (Table 1, entry 1–3). CyJohnPhos and DavePhos⁴⁵ gave similar assay yields (89–90 % AY) with cataCXium PCy lagging (45 % AY). Changing the solvent from THF to dimethoxyethane (DME) resulted in an increase in AY to 98 % with DavePhos (Table 1, entry 4) and no change with CyJohnPhos (89 % AY, Table 1, entry 5).

Attempts at lowering the ligand loading and the temperature were found to be successful with optimization at a 5:10 mol % Pd:L ratio and a 50 °C reaction temperature (Table 1, entries 6–9). When the ratio of Grignard reagent to electrophile (hereafter referred to as Mg: ArX) was reduced to 2.0, the yield dropped to 75 % (Table 1, entry 10). Finally, further optimization for reaction time found that the reaction was complete within 4 h under the optimized conditions (Table 1, entry 7) and a 99 % isolated yield was determined (Table 1, entry 11).

Table 1. Optimization of cross-coupling between 1a and 2a.a

6

7

8

9

10

11

DavePhos

DavePhos

DavePhos

DavePhos

DavePhos

DavePhos

DME

DME

DME

DME

DME

DME

^a Reactions conducted on a 0.1 mmol scale at 0.1 M. ^b Assay yields determined by ¹H NMR spectroscopy of the crude reaction mixture using CH₂Br₂ as the internal standard. ^c Isolated yield after chromatographic purification and 4 h reaction time.

5/10

5/10

5/10

2.5/5

5/10

5/10

As outlined in Figure 1 and elsewhere, 46 oxidative additions are known to be dependent on the electronic nature of the arvl group, with electron poor aryl halides undergoing faster oxidative addition than analogous electron rich derivatives. Thus, various aryl fluorides were employed with phenylmagnesium bromide to determine if the reaction was general with respect to Ar-F (Table 2). Aryl fluorides bearing weak electron donating groups at the para position, such as phenyl, or strong electron donating groups, like methoxy and N,N-dimethylamino, provided high yields of the products 3a, 3b, and 3c in 99, 95, and 91 %, respectively. Electron withdrawing 3-fluoroanisole was a viable substrate, furnishing the product 3d in 99 % yield. Interestingly, when strong electron withdrawing groups at the para position were used, such as trifluoromethyl (1e), no coupling products were observed. In contrast, use of NIXANTPHOS (7.5 mol %) at 80 °C for 12 h furnished the coupling product 3e in 78 %. Sterically hindered aryl fluorides, such as 1-fluoro naphthalene or 2-methyl and 2-methoxy 1-fluorobenzene, were also tested but only gave moderate yields (around 50 %) under the standard conditions. Furthermore, it proved difficult to isolate the products by chromatography due to their nonpolar nature. When a higher reaction temperature (80 °C) and an alternative Grignard reagent (4-methoxyphenylmagnesium bromide, to aid in chromatographic isolation) were used, the desired products 3f-3h were isolated in 73-96 % yield. Heterocyclic substrates, 1-(4-fluorophenyl)-1*H*-pyrrole including (1i),(1j), 5-fluorobenzofuran 6-fluoroquinoline (1k)and 5-fluorobenzothiophene (11) were examined, but only 1-(4-fluorophenyl)-1*H*-pyrrole gave product (3i, 91 % yield)

using DavePhos. Switching the ligand to CyJohnPhos allowed for the remaining heterocyclic substrates to be successfully coupled in 52–59 % yields (3j–3l). Finally, substrates bearing hydroxyl (1m) and alkynyl (1n) groups were also examined. DavePhos again gave low yields for these substrates but the related CyJohnPhos provided products 3m and 3n in 44 and 55 % yields, respectively.

80

50

25

50

50

50

100%

100%

33%

74% 75%

100% (99% °)

2.2 Mechanistic Insights

1:2.5

1:2.5

1:2.5

1:2.5

1:2

1:2.5

In Pd-mediated KTC cross-coupling chemistry, the accepted turnover-limiting step (TLS) involves the oxidative addition of the Ar–X prior to transmetallation by a Grignard reagent. However, the inability of typical $L_1Pd(0)$ complexes to oxidatively add Ar–F bonds prompted further investigation into the means by which the present system is able to mediate this transformation.

Competition experiments were conducted using equimolar mixtures of 4-tert-butoxychlorobenzene and 4-methoxyfluorobenzene with varying amounts of phenylmagnesium bromide. These were catalyzed by 5 mol % Pd(OAc)₂ and 10 mol% DavePhos in 1 mL DME at 50 °C for 4 h (Table 3). If the Grignard reagent is not involved in (or before) the TLS, then we expect to see a clear preference for the activation of the aryl chloride at all Mg: ArX ratios, as aryl chloride will undergo oxidative addition faster than the aryl fluoride.

There were several interesting observations from these competition experiments. First, at Mg: ArX ratios of 0.1:1, we only observed the C–Cl bond activation product, **3p**. Second,

the ratio of C–F activation product (**30**) to C–Cl activation product (**3p**) *increases* when Mg: ArX ratios are increased from 0.1:1 to 1:1, with rates of C–F to C–Cl activation becoming equitable above Mg: ArX ratios of ~0.75:1. Third, when the reaction was run under the optimized conditions, with a Mg: ArX ratio of 2.5:1, the ratio of C–F to C–Cl activation is 1:1. We conducted time course experiments tracking the formation of **3o** from Ar–F and **3p** from Ar–Cl in parallel reactions under the optimized conditions. At a Mg: ArX ratio of 1:1, a faster reaction rate was observed for Ar–Cl (1 h, 27%; 4 h, 50%) compared to Ar–F (1 h, 20%; 4 h, 38%) (Figure 3). However, when the Mg: ArX ratio was increased to 2.5:1, the rates of both reactions increased and became more equal between Ar–Cl (1 h, 46%; 4 h, 91%) and Ar-F (1 h, 45%; 4 h, 100%) (Figure 3).

Taken together, these data suggest that a non-traditional KTC mechanism is being accessed at higher ratios of Mg: ArX concentrations. This dependence on the ratio of concentrations indicates that it may be possible for both PhMgBr and Ar–X to associate with Pd(0), with Ar–X association leading to a traditional KTC mechanism for Ar–Cl, which is favored at low Mg: ArX ratios, and PhMgBr association leading to an alternative pathway for both Ar–Cl and Ar–F at high Mg: ArX ratios.

Table 2. Examples of aryl fluorides suitable for cross-coupling with aryl Grignard reagents. a,b

^a Reactions conducted on a 0.1 mmol scale at 0.1 M. ^b Isolated yields after chromatographic purification. ^c NIXANTPHOS (7.5 mol %), 80 °C, 12 h. ^d 4-methoxyphenylmagnesium bromide (2.5 equiv.), 80 °C, 12 h. ^e 80 °C, 12 h. ^f Pd(OAc)₂ (10 mol %), CyJohnPhos (20 mol %), 80 °C, 12 h and 3.5 equiv Grignard reagent for 31.

2.3 Computational Study

We next turned to DFT computations to inform our understanding of the manner in which this system is able to promote Ar–F cross coupling. Of the 48 screened phosphine ligands, the three that were most successful share a common structural motif that includes two cyclohexyl groups and one biphenyl-type unit. We chose one of these (DavePhos) as a case study for identifying a mechanism that is able to account for the experimental data.

Table 3. Aryl fluoride and aryl chloride competition experiments as a function of Mg: ArX ratio.

Entry	PhMgBr:ArX	30 (mmol)	3p (mmol)	30:3p
1	0.1:1	0.0000	0.0019	0.00
2	0.25:1	0.0039	0.0114	0.34
3	0.5:1	0.0162	0.0248	0.66
4	0.75:1	0.0243	0.0225	1.08
5	1:1	0.0416	0.0385	1.08
6	1.5:1	0.0446	0.0425	1.05
7	2:1	0.0485	0.0462	1.05
8	2.5:1	0.0447	0.0453	0.99

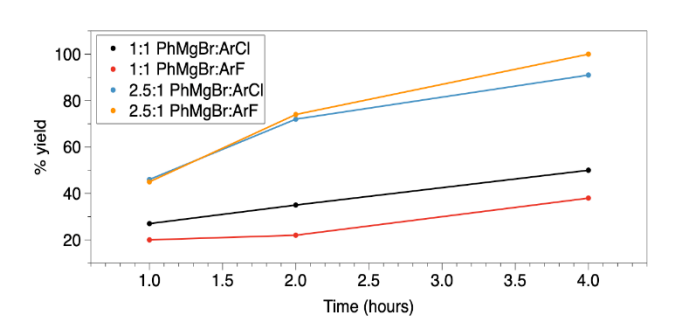


Figure 3. Parallel-reaction monitoring at Mg: ArX ratios of 1:1 and 2.5:1.

The monophosphine Pd(0) complex (DavePhos)Pd (4) was found to be stabilized by an intramolecular η²-π-interaction between Pd and the *o*-aryl group of the phosphine (denoted as Ar_P), as previously noted by Buchwald⁴⁹ (Figure 4). For complex 4, this interaction creates a 14 e⁻ metal center and provides a 17 kcal/mol stabilization (see SI). Minor changes to the Pd–P bond length and the Pd–P-C_{ipso} angle compared to those in the 12 e⁻ L₁Pd isomer indicate that Ar_P binding to Pd does not result in significant structural changes to the ligand backbone. In addition to Ar_P, the coordination of other donors present in the reaction mixture (DME, DavePhos, arenes) provided stabilization with respect to 4 (see SI). These include the adduct of 4 with the biphenyl C–C coupling product 4-methoxybiphenyl (30), which forms the Pd(0)-biphenyl adduct 5. The free energy of 5 plus those of PhMgBr, ArCl, and ArF is

used to define the zero point on the energy surfaces described below.

Figure 4. Proposed traditional KTC cross-coupling catalytic cycle.

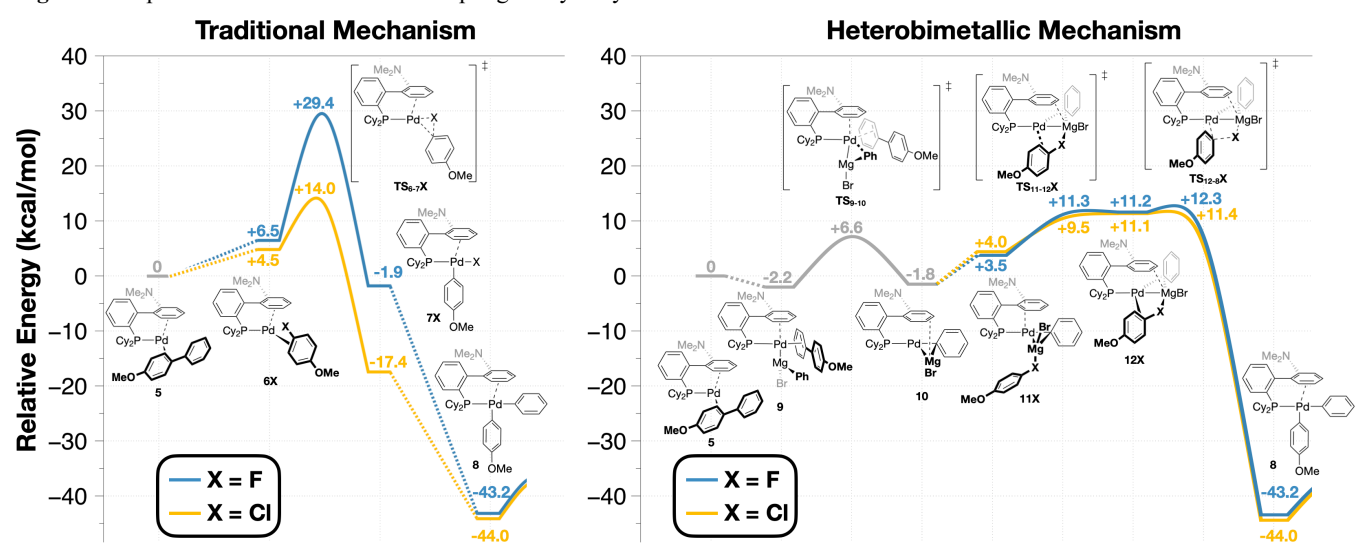


Figure 5. Potential energy diagrams for traditional (left) and heterobimetallic (right) KTC cross-coupling catalytic cycles. Dashed lines connect local minima; smooth lines connect local minima with transition states.

The traditional cross-coupling catalytic cycle involves the formation of an adduct between an aryl halide and the Pd(0) species 4 (Figure 4). This could be envisioned to occur along the catalytic cycle via either dissociation of the biphenyl product (30) from 5, followed by association of ArX, or by associative substitution of ArX for 3o. Stahl, Landis, and co-workers have used kinetic experiments and DFT studies to show that a 14 e- Pd complex undergoes associative ligand exchange involving η^2 -bound olefins, with activation barriers of 10–14 kcal/mol.⁵⁰ In the present example, attempts to locate transition states for either dissociative or associative ligand exchange processes were unsuccessful. The coordination sphere about Pd in 5 is too hindered to accommodate an additional π -arene interaction, but ring-slippage of biphenyl or dissociation of Ar_P could be envisioned to create enough space for binding ArX prior to dissociation of 30. A dissociative pathway is also feasible; loss of 30 from 5 is endergonic by 10.0 kcal/mol and requires minimal reorganization of the coordination sphere about Pd, indicating that 10 kcal/mol may be considered an upper bound for the activation energy required to form a Pd(0) complex of ArX from 5.

The ligand exchange process yields the π-ArX complexes **6X** (**X** = **F**, **Cl**), which exhibit Pd–C_{ArX} distances of *ca*. 2.21 Å (**6Cl**) and 2.40 Å (**6F**) as well as η² Pd-Ar_P distances of *ca*. 2.83 Å (**6Cl**) and 2.81 Å (**6F**). The subsequent Ar–X oxidative addition transition states (**TS**₆₋₇**X**) were located at +14.0 (**TS**₆₋₇**Cl**) and +29.4 (**TS**₆₋₇**F**) kcal/mol from **6X** (Figure 5, left). The significant difference in energy between the rate-determining steps for this catalytic cycle are in line with the conventional understanding that monophosphine Pd complexes undergo facile Ar–Cl oxidative addition and slow Ar–F cleavage. The geometries of **TS**₆₋₇**X** exhibit typical three-centered TS character, in line with significant Pd–C and Pd–X bond formation as well as C–X bond cleavage.

The oxidative addition steps lead to the formation of Ar–Pd(II)–X compounds (7X). Evaluation of the various possible isomers of $TS_{6-7}X$ and 7X revealed both a kinetic and thermodynamic preference for placing the halide *trans* to the phosphine. The products 7CI (–21.9 kcal/mol from 6CI) and 7F (–8.4 kcal/mol from 6F) exhibited T-shaped core geometries with added η^2 -cation- π interactions between Pd and Ar_P, which

complete square-planar coordination environments about the Pd(II) metal centers.

Figure 6. Proposed heterobimetallic catalytic cycle.

Repeated attempts to locate a transition state for transmetallation (TS₇₋₈X) were unsuccessful. Transmetallation has been shown to be turnover-limiting for Suzuki³² and Stille⁵¹ couplings, but oxidative addition is thought to be turnover-limiting for the more closely related Negishi coupling reactions.⁵²⁻⁵³ For transmetallation to be turnover-limiting, the putative TS₇₋₈X steps would need to lie >30 kcal/mol above 7X. For comparison, the computed barrier to transmetallation in the aforementioned Negishi cycle is *ca.* 10 kcal/mol from the oxidative addition product.

The product of transmetallation with PhMgBr yields the Ar–Pd(II)–Ph species, **8**, and MgBrX. Compound **8** again exhibits an η^2 -cation- π interaction between Pd and Ar_P (Pd–Ar_P = ca. 2.77 Å). Reductive elimination (**TS**₈₋₅) is calculated to be facile (ca. –40 kcal/mol versus **6**) *en route* to regenerating the Pd(0) species **5**, which closes the catalytic cycle.

The calculations thus predict that the rate of the traditional KTC pathway is turnover-limited at the oxidative addition step during both Ar–F and Ar–Cl activation. The predicted kinetic preference for Ar–Cl bond activation ($\Delta\Delta G^{\ddagger}=15.4$ kcal/mol) contrasts, however, with the competitive Ar–F and Ar–Cl bond activation observed experimentally, suggesting that an alternative pathway is likely operative. The traditional KTC pathway also does not account for the experimental observation that Ar–F cross-coupling depends on the relative concentration of Grignard to electrophile, which suggests that the Grignard reagent may compete with the electrophile for binding to Pd(0).

Crystallographic examples are known of alkyl magnesium complexes forming Lewis acid-base adducts with Fe, Co, Ni, and Cu. 54-58 In most cases, the alkyl group stabilizes the heterobimetallic core by bridging between the two metal centers $(d_{M-Mg}=ca.\ 2.6\ \text{Å})$. During the final stages of preparation of this manuscript, Crimmin and coworkers reported hexagonal planar palladium $Pd(H)_3[Mg(nacnac)]_3$ complexes, including their characterization by X-ray diffraction. The Pd–Mg bonds in these compounds range from 2.485(1) to 2.567(1) Å. Addition of phosphines to the hexagonal planar complex resulted in formation of $R_3P-Pd[\eta^2-H-Mg(nacnac)]_2$, with the

phosphine and hydrides in the equatorial plane. These are the first examples of Pd–Mg adducts characterized structurally. The interaction of the Mg and Pd in such complexes supports our speculation that bimetallic Pd–Mg interactions are viable in the non-traditional pathway of the KTC-coupling of aryl fluorides described herein.

We and others have previously shown that cation- π interactions can be used to house Lewis acidic metals near a Pd center, and Mg(II) has been shown to form intramolecular cation- π interactions.⁵⁵⁻⁵⁸ In addition, a handful of reports of heterobimetallic activation of Ar-X electrophiles have been described in the literature. The most salient example involved a Ni-Mg heterobimetallic complex.³⁹⁻⁴⁰ In this case, the proposed reaction coordinate included a nickel hydroxyphosphine complex, the alkoxy group forming a bridge between the Pd and Mg (Figure 2c and Figure 7). The close proximity of the two metal centers allowed for the activation of Ar-X substrates through the concerted delivery of X to Mg and Ar to Ni (Figure 7). Transition states were identified for $X = OP(O)(OMe)_2$, OC(O)NMe2, OMe, and SMe, but attempts to locate transition states for aryl halide activation (X = F, Cl, Br) were unsuccessful.39-40

$$\begin{array}{c} Ph_{2}P \\ Ni \\ MgY \end{array} \begin{array}{c} Ph_{2}P \\ Ni \\ MgY \end{array} \begin{array}{c} Ph_{2}P \\ Ni \\ MgXY \end{array} \begin{array}{c} Ph_{2}P \\ Ni \\ MgXY \end{array} \begin{array}{c} Ph_{2}P \\ MgXY \end{array}$$

Figure 7. Mg-Ni cooperative activation of ArX proposed by Nakamura and co-workers.³⁹

With DavePhos as a supporting ligand, the interaction between Pd(0) (5) and PhMgBr was computed to be mildly exergonic ($\Delta G = -2.2 \text{ kcal/mol}$) on formation of an association complex (9). The Grignard is Mg-bound to Pd, leading to a Pd–Mg distance of 2.57 Å. A transition state corresponding to both binding of the Grignard Cipso carbon to Pd and concurrent dissociation of the η^2 -bound biphenyl unit was located at +6.6 kcal/mol vs. 5. The product of this ligand exchange process is a heterobimetallic palladate species, 10 (-1.8 kcal/mol; Figure 6). Compound 10 features a Pd-Mg distance of 2.44 Å, which, like 9, is similar to those observed in the structures reported by Crimmin.⁵⁹ The Pd-Mg interaction in **10** is supported with both a μ -phenyl bridge (Pd–C_{ipso} = 2.11 Å, Mg- C_{ipso} = 2.35 Å; Pd- C_{ipso} - C_{para} = 158.2°) and an η^2 cation- π interaction between Mg and the biphenyl portion of the phosphine ligand. The Mg– C_{π} distances of ca. 2.79 Å are comparable with crystallographically characterized compounds that share the η^2 -cation- π motif (Mg-C $_\pi$ distances of ca. 2.62 Å).54

Considering that the KTC cross-coupling reaction produces magnesium halide salts, we also investigated the binding of alternative Mg-containing salts to Pd(0) to form analogs of **10** (see SI). The formation of Pd(0)–MgXY complexes (MgXY = MgBr₂, MgF₂, MgBrF) were found to be endergonic from **5** by >10 kcal/mol. These results, compared to the exergonic formation of **10** from **5**, suggest that the μ -Ph linkage in **10** provides a particular advantage in the present system.

The formally anionic Pd(0) center of 10 adopts a T-shaped geometry, with the μ -phenyl ipso carbon located trans to the phosphine (<P-Pd-C_{ipso} = $\overline{170.3}^{\circ}$) and the Mg center *cis* to the phosphine (<P-Pd-Mg = 117.8°). This geometry did not provide a direct pathway for approach of ArX that would allow for cooperative action by Pd and Mg; however, it was found that halide-binding of ArX to Mg was viable to give a product that was mildly endergonic (11X; +3.5/+4.0 kcal/mol for X = F/Cl). These complexes displayed a similarly inaccessible core geometry as 10, but the search for a C-X bond activation pathway was advanced by scanning the P-Pd-C_{ipso} angle on 10. Doing so from 175° to 100° revealed a flat potential energy surface that results from the lack of directional bonding at Pd(0)(see Figure 8). The binding of Ar_P migrates through the scan, from an η^2 interaction with Mg in the ground state to an η^2 π interaction with Pd(0) at P–Pd– $C_{ipso} = 100^{\circ}$. The structure with the most acute angle lies a mere 4.5 kcal/mol higher in energy than the ground state geometry and contains space for heterobimetallic Ar–X binding.

$$\begin{array}{c} \text{Me}_2\text{N}, \\ \text{Cy}_2\text{P} - \text{Pd} - \text{C}_{\text{ipso}} = 175^{\circ} \\ E_{\text{rel}} = 0 \text{ kcal/mol} \end{array}$$

Figure 8. Relative energies of **10** in its ground state geometry (left) and with a constrained P–Pd–C_{ipso} angle of 100° (right).

With this in mind, scanning the Pd– $C_{ipso,ArX}$ distance of **11X** identified late transition states for formation of a π -bond between Pd and ArX. This step takes advantage of the shallow potential energy surface defined by the P–Pd– $C_{ipso,Mg}$ angle to create space for interaction between the aryl π -system and Pd

but appears to be guided by the interaction between Mg and X, as the Mg–X distances are nearly invariant from the ground state to the transition state. The energy of this transition state was determined to be *ca.* 10 kcal/mol, which places it on par with the C–Cl activation energy in the tradition KTC pathway described above.

Relaxation from this transition state toward the formation of the Pd–ArX π -bond reveals a high-energy intermediate (12X) characterized by η^2 π -bonding to Pd, a dative Mg–X interaction (Mg–Cl = 2.57 Å; Mg–F = 2.14 Å), and significant activation of the Ar–F bond. Ar_P returns to Mg in 12X, forming cation- π interactions at distances of ca. 2.92 Å (Cl) and 2.83 Å (F). The modest increase in free energy on formation of 12X (+13.6 kcal/mol vs. {10 + Ar–X}) masks the substantial activation of the aryl halides, which both exhibit 0.11 Å increases in the Ar–X bond distances and pyramidalization of the ArX ipso carbon (sum of angles about C_{ipso} = 343.2°; <Pd- C_{ipso} - C_{para} = 107.3°).

Nakamura and co-workers used constrained geometry scans to support the notion that aryl halide bond activation is nearly barrierless in the Ni: Mg heterobimetallic system. In the present system, the transition states for Ar-X bond cleavage (TS₁₀₋₈X) were located and found to exhibit exceedingly small activation energies with respect to 12X: +0.2 kcal/mol for TS₁₂₋₈Cl and +1.1 kcal/mol for TS₁₂₋₈F. The structures of TS₁₂₋₈X are similar to those of 12X, in accord with Hammond's postulate (Figure 9). Both of the Ar–X distances in TS₁₂₋₈X are elongated by 0.32 Å from 12X, while the Mg-X and Pd-C_{ipso(ArX)} distances decrease by 0.11 Å, as expected for Ar–X bond breaking and Pd-Ar/Mg-X bond formation. We note that Ar_P retains η^2 cation- π interactions of ca. 2.9 Å with Mg in the transition states. We were unable to locate intermediates following TS₁₂₋₈X that retain MgBrX in the coordination sphere of Pd. Presumably, oxidation to Pd(II) weakens the Pd-Mg interaction such that salt loss requires a negligible amount of energy. The resulting Ph-Pd(II)-Ar species (8, described above) undergoes reductive elimination through the previously described three-center transition state (TS₈₋₅), calculated to lie >45 kcal/mol lower in energy than TS₁₂₋₈X (see SI).

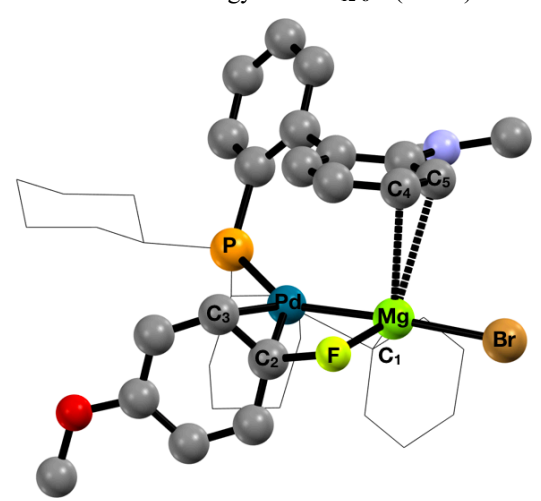


Figure 9. DFT optimized structure of **TS**₁₂₋₈**F**; all hydrogen atoms were removed for clarity. Important bond lengths (Å) and angles (deg): Pd–C1 2.166, Pd–C2 2.076, Pd–C3 2.474, Pd–Mg 2.610, Pd–P 2.381, F–C2 1.683, Mg–C1 2.320, Mg–C4 2.798, Mg–C5 3.044, F–Mg–Br 107.1, Pd–Mg–C1 51.7, C2–F–Mg 96.3.

It was found experimentally that increasing the Grignard concentration mitigated the difference in rates of formation of Ar–F and Ar–Cl coupling products. This suggests that at low Mg : ArX ratios, the traditional KTC pathway is favoured, yielding higher proportions of Ar–Cl over Ar–F activation products. However, with high Mg : ArX ratios, the available Pd(0) in solution accesses a heterobimetallic pathway. This is consistent with the results of the competition experiment, which found that Ar–F and Ar–Cl activation occurred at comparable rates under conditions with high Mg:ArX ratios. It should be noted that the heterobimetallic mechanism offers a significant stabilization in Ar–F bond activation compared to the traditional KTC mechanism (*i.e.* TS₆₋₇F vs. TS₁₂₋₈F). The ΔG^{\ddagger} for the Ar–F bond cleavage step was found to decrease by 16.9 kcal/mol in the heterobimetallic mechanism.

2.4 Experimental support for a heterobimetallic mechanism.

Additional experimental work was used to further probe the heterobimetallic reaction mechanism that is proposed to occur at elevated Mg: ArX ratios. We envisioned that the different steric profiles between the traditional KTC mechanism and the heterobimetallic pathway might provide an opportunity to probe these competing modes of oxidative addition. The rates of traditional KTC cycles are known to show little variation in response to the steric profile of the electrophile.⁴⁹ In contrast, the constrained environment imposed by the heterobimetallic architecture might be expected to inhibit the binding of sterically hindered aryl halides. To probe this hypothesis, 2,6-dimethyl-1-fluorobenzene and 3,5-dimethyl-1-fluorobenzene were evaluated as substrates under the optimized reaction conditions described above, with Mg: ArX = 2.5 : 1. The use of 3,5-dimethyl-1-fluorobenzene resulted in a slower reaction rate compared to 4-phenyl-1-fluorobenzene (80% vs. 99% yield after 4 h), and the use of 2,6-dimethyl-1fluorobenzene halted the reaction entirely.

This outcome was further used to support the notion that the Mg: ArX ratio controls access to either the traditional KTC or heterobimetallic mechanisms. With the 2,6-dimethyl-1halobenzenes as substrates, we anticipated that low Mg: ArX ratios would provide cross-coupling with both substrates, with a preference for Ar-Cl activation through the traditional KTC pathway, but at high Mg: ArX ratios, 2,6-dimethyl-1chlorobenzene would join 2,6-dimethyl-1-fluorobenzene as an inactive substrate under these conditions. Indeed, at a Mg: ArX ratio of 0.25: 1, coupling to Ar-Cl was favored, forming the cross-coupling product in 23 % yield, compared to 7 % yield when the Ar-F was evaluated under identical conditions (Figure 10). When the Mg: ArX ratio was raised to 1:1, both yields decreased dramatically, resulting in 2% and 0% yield for Ar-Cl and Ar-F, respectively. At a Mg: ArX ratio of 2.5:1, no product was observed for either substrate. These findings corroborate the hypothesis that at low Mg: ArX ratios, the cross-coupling reaction proceeds through a traditional KTC mechanism, with coupling to Ar-Cl proceeding more quickly. This is consistent with literature reports, which indicate that o-dimethyl substitutions provide little steric hinderance to oxidative addition at low-coordinate Pd(0).⁴⁹ These results also comport with the data presented in Table 3 that show a similar ratio of Ar-F: Ar-Cl activation products (0.34) under a Mg: ArX ratio of 0.25 : 1.00. At Mg : ArX ratios \geq 1, the inability of the 2,6-dimethyl substrates to undergo cross-coupling supports the view that this system is accessing a unique mechanism that both prevents access to the traditional KTC pathway and presents a pathway that is susceptible to the presence of *o*-substitutions on the electrophile.

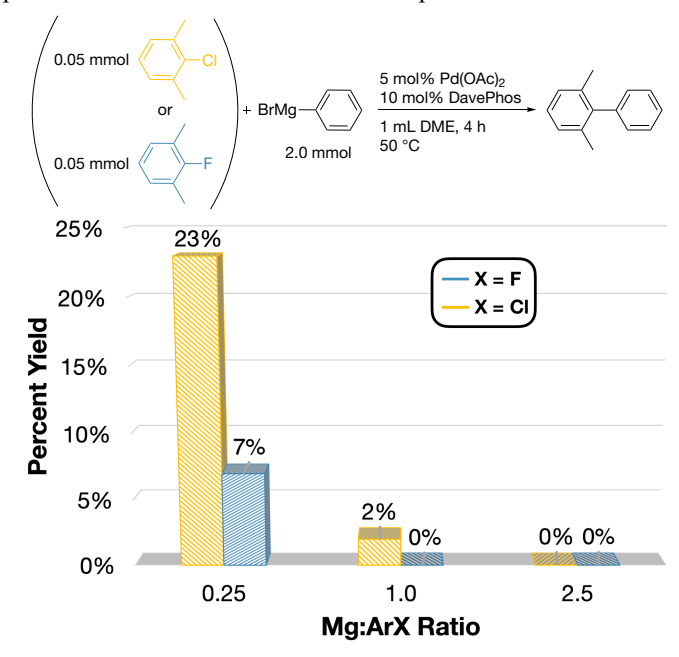


Figure 10. Parallel-reaction competition experiments at Mg: ArX Ratios of 0.25 : 1, 1 : 1 and, 2.5 : 1 using 2,6-dimethyl-1-fluorobenzene or 2,6-dimethyl-1-chlorobenzene.

In order to probe the origin of the steric interaction that is causing the dimethyl-substituted substrates to diverge from the reactivity described above, we computed the energies of 12F-xyl and TS₁₂₋₈F-xyl, in which 2,6-dimethyl-1-fluorobenzene is substituted for the 4-methoxy-1-fluorobenzene substrate of 12F and TS₁₂₋₈F. The modest increase in ground state and transition state energies (+13.2 and +15.8 kcal/mol, respectively, vs. 5) indicate that this step is not responsible for preventing the formation of cross-coupled products under high Mg: ArX ratios (Figure 10). This information, coupled with the observation that product is formed under low Mg: ArX ratios, led us to reason that i) Grignard effectively outcompetes ArX for Pd(0), and ii) that the steric profile of the 2,6-dimethyl-halobenzenes prevents them from forming 12X.

On evaluation of the full energy surface provided in Figure 5, we are left with the conclusion that the heterobimetallic mechanism is governed by either the formation of the highenergy intermediate 12X (TS₁₁₋₁₂X) or the Ar-X bond cleavage process (TS₁₂₋₈X), depending on the steric profile of the electrophile. For the p-OMe substrates these transition states are nearly equal in energy, but the experimental data indicate that $TS_{11-12}X$, which involves formation of a Pd- π -complex with the aryl halide, becomes turnover-limiting when the 2,6-C₆H₃-Me₂ substitution pattern is present. With less sterically demanding electrophiles, the C-X activation energies of the heterobimetallic pathways are similar to the C-Cl activation energy of the traditional KTC pathway, meaning the species that exist on these energy surfaces prior to Ar-X bond activation would be in equilibrium with one another. This fits with the experimental observation that Ar-F bond activation does not occur until roughly equal measures of Grignard and ArX are present in solution. Even so, the tendency toward access to the heterobimetallic activation pathway is nonnegligible, as noted from the ratios of **30**: **3p** listed in Table 3. The 0.34: 1.00 ratio of products, for example, obtained under reaction conditions that used a Mg: ArX ratio of 0.25: 1.00, may be thought to represent equal access to the two pathways, if one assumes that all of the Ar-F activation is from the heterobimetallic pathway and that the Ar-F and Ar-Cl bond activation steps are equivalent in energy in this new heterobimetallic mechanism. This preference for the heterobimetallic pathway would then result from the lower relative energies of 9 and 10 (ca. -2 kcal/mol) compared to the endergonic Pd-ArX intermediates (6X, ca. +5 kcal/mol) observed on the traditional KTC pathway. The equilibrium population of the species along the heterobimetallic pathway will be greater. With similar energy barriers to Ar-X activation via either pathway, the thermodynamic preference for the heterobimetallic intermediates will lead to greater usage of the Pd-Mg architecture for C-X bond activation.

Finally, the proposed Pd-Mg heterobimetallic structure was supported through the use of a novel phosphine ligand, Cy₂P(o-Bn-C₆H₄), in which an *ortho* position on the aryl ring of Cy₂PPh was substituted with a benzyl group. Under the optimized reaction conditions described above, this ligand provided a 68% yield of Ar-F cross-coupling (Figure 11). Additional support for the ability of Cy₂P(o-Bn-C₆H₄) to mediate a heterobimetallic mechanism similar to TS₁₂₋₈F was obtained using DFT computations. A transition state (TS₁₂₋₈F-oBn) was identified with the Cy₂P(o-Bn-C₆H₄) ligand and found to closely match the structure of TS₁₂₋₈F (Figure 12). TS₁₂₋₈F-oBn exhibits an Ar-F distance of 1.690 Å (vs. 1.683 Å in TS₁₂₋₈F), along with a Mg-F distance of 1.993 Å (1.987 Å for TS₁₂₋₈F) and a Pd-C_{ipso(ArX)} distance of 2.061 Å (2.076 Å for TS₁₂₋₈F). Ar_P was found to retain an η^2 cation- π interaction of ca. 2.9 Å with Mg in both $TS_{12-8}F$ and $TS_{12-8}F$ -oBn.

Figure 11. Reactions with modified phosphines.

Further modifications to the phosphine revealed the importance of both the cyclohexyl and pendant aryl moieties; use of either Ph₂P(*o*-Bn-C₆H₄) or Cy₂P(*o*-C₆H₄-Me) resulted in comparable activity to the phosphine-free conditions (20% and 18% yield, respectively). We propose that the aliphatic cyclohexyl groups are necessary for creating an electron rich Pd(0) center, and that the *o*-Bn group aids the electron rich metal in retaining Mg in the coordination sphere of Pd. The diminished yield observed for Cy₂P(*o*-Bn-C₆H₄) compared to CyJohnPhos/DavePhos suggests, however, that the heterobimetallic activation of Ar–X is highly sensitive to the manner in which the Lewis acid is supported and positioned.

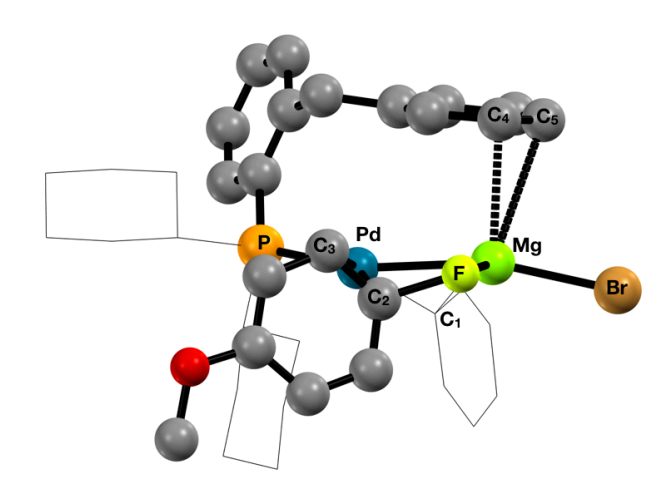


Figure 12. DFT optimized structure of $TS_{12-8}F$ -oBn; all hydrogen atoms were removed for clarity. Important bond lengths (Å) and angles (deg): Pd–C1 2.158, Pd–C2 2.061, Pd–C3 2.405, Pd–Mg 2.662, Pd–P 2.386, F–C2 1.690, Mg–C1 2.294, Mg–C4 2.776, Mg–C5 3.062, Mg–F 1.993, F–Mg–Br 105.9, Pd–Mg–C1 51.1 C2–F–Mg 95.0.

3. Conclusion

The most significant accomplishment of this work is that a mechanism for oxidative addition of aryl chlorides and fluorides has been identified that proceeds via a bimetallic Pd-Mg transition state. A range of arvl fluorides with different electronic and steric profiles lead to products in moderate to excellent yields. A computational study was used to evaluate two possible reaction mechanisms. In sub-stoichiometric Mg: ArX ratios, it is proposed that the electrophile outcompetes the Grignard for binding to Pd(0). This leads to a traditional KTC pathway involving oxidative addition of the electrophile, followed by transmetallation from the Grignard reagent. However, due to the Ar_P-assisted binding of Mg, coordination of Grignard competes for Pd(0) at elevated Mg: ArX ratios, such as those usually employed in KTC coupling reactions. The resulting heterobimetallic complex appears to be equally competent at Ar-F and Ar-Cl activation, while providing a substantial decrease in the activation energy for Ar-F compared to the traditional oxidative addition pathway. The cooperativity of Mg and Pd was facilitated by a cation- π interaction with a biphenyl group on the phosphine. This interaction supported the close proximity of Mg and Pd, which was shown to be integral to efficient aryl halide bond activation via the bimetallic pathway. Further exploitation of this bimetallic cooperativity is underway.

ASSOCIATED CONTENT

Supporting Information

The Supporting Information is available free of charge on the ACS Publications website. Procedures, characterization data for all new compounds and calculation for mechanisms (PDF).

AUTHOR INFORMATION

Corresponding Author

* E-mail: tomson@upenn.edu (N.C.T.).

E-mail: pwalsh@sas.upenn.edu (P.J.W.).

Author Contributions

[‡] These authors contributed equally. (C.W. and S.P.M.)

Notes

The authors declare no competing financial interest.

ACKNOWLEDGMENT

N.C.T. acknowledges the National Institute of General Medical Sciences (NIGMS) of the National Institutes of Health (NIH) for support of this work under award number R35GM128794 and the Charles E. Kaufman Foundation, a supporting organization of The Pittsburgh Foundation, for support in the form of a New Investigator Research Grant (KA2016-85227). P.J.W. thanks the National Science Foundation (CHE-1902509) and the Petroleum Research Fund managed by the American Chemical Society (PRF 59570-ND1) for financial support.

REFERENCES

- Kiplinger, J. L.; Richmond, T. G.; Osterberg, C. E., Activation of Carbon-Fluorine Bonds by Metal Complexes. *Chem. Rev.* 1994, 94 (2), 373-431.
- O'Hagan, D., Understanding organofluorine chemistry. An introduction to the C-F bond. *Chem. Soc. Rev.* 2008, 37 (2), 308-319.
- Amii, H.; Uneyama, K., C-F Bond Activation in Organic Synthesis. Chem. Rev. 2009, 109 (5), 2119-2183.
- Clot, E.; Eisenstein, O.; Jasim, N.; Macgregor, S. A.; McGrady, J. E.; Perutz, R. N., C-F and C-H Bond Activation of Fluorobenzenes and Fluoropyridines at Transition Metal Centers: How Fluorine Tips the Scales. Acc. Chem. Res. 2011, 44 (5), 333-348
- Ahrens, T.; Kohlmann, J.; Ahrens, M.; Braun, T., Functionalization of Fluorinated Molecules by Transition-Metal-Mediated C–F Bond Activation To Access Fluorinated Building Blocks. Chem. Rev. 2015, 115 (2), 931-972.
- Shen, Q.; Huang, Y.-G.; Liu, C.; Xiao, J.-C.; Chen, Q.-Y.; Guo, Y., Review of recent advances in CF bond activation of aliphatic fluorides. *J. Fluor. Chem.* 2015, 179, 14-22.
- Utsumi, S.; Katagiri, T.; Uneyama, K., Mg—Cu bimetal system for selective CF bond activation. J. Fluor. Chem. 2013, 152, 84-89.
- 8. Doster, M. E.; Johnson, S. A., Selective C–F Bond Activation of Tetrafluorobenzenes by Nickel(0) with a Nitrogen Donor Analogous to N-Heterocyclic Carbenes. *Angew. Chem. Int. Ed.* **2009**, *48* (12), 2185-2187.
- Träff, A. M.; Janjetovic, M.; Ta, L.; Hilmersson, G., Selective C– F Bond Activation: Substitution of Unactivated Alkyl Fluorides using YbI₃. Angew. Chem. Int. Ed. 2013, 52 (46), 12073-12076.
- Tasker, S. Z.; Standley, E. A.; Jamison, T. F., Recent Advances in Homogeneous Nickel Catalysis. *Nature* 2014, 509 (7500), 299-309.
- Tobisu, M.; Xu, T.; Shimasaki, T.; Chatani, N., Nickel-Catalyzed Suzuki–Miyaura Reaction of Aryl Fluorides. *J. Am. Chem. Soc.* 2011, 133 (48), 19505-19511.
- Littke, A. F.; Fu, G. C., Palladium-catalyzed coupling reactions of aryl chlorides. *Angew. Chem., Int. Ed.* 2002, 41 (22), 4176-211.
- Liu, X.-W.; Echavarren, J.; Zarate, C.; Martin, R., Ni-Catalyzed Borylation of Aryl Fluorides via C–F Cleavage. *J. Am. Chem. Soc.* 2015, 137 (39), 12470-12473.
- 14. Li, J.; Wu, C.; Zhou, B.; Walsh, P. J., Nickel-Catalyzed C(sp³)–H Arylation of Diarylmethane Derivatives with Aryl Fluorides. *J. Org. Chem.* **2018**, *83*, 2993–2999.
- Dankwardt, J. W., Transition metal catalyzed cross-coupling of aryl Grignard reagents with aryl fluorides via Pd- or Ni-activation of the C-F bond: an efficient synthesis of unsymmetrical biaryls application of microwave technology in ligand and catalyst screening. J. Organomet. Chem. 2005, 690 (4), 932-938.

- Cargill, M. R.; Sandford, G.; Tadeusiak, A. J.; Yufit, D. S.; Howard, J. A. K.; Kilickiran, P.; Nelles, G., Palladium-Catalyzed C-F Activation of Polyfluoronitrobenzene Derivatives in Suzuki-Miyaura Coupling Reactions. *J. Org. Chem.* 2010, 75 (17), 5860-5866.
- Bahmanyar, S.; Borer, B. C.; Kim, Y. M.; Kurtz, D. M.; Yu, S., Proximity Effects in the Palladium-Catalyzed Substitution of Aryl Fluorides. Org. Lett. 2005, 7 (6), 1011-1014.
- Ishikawa, S.; Manabe, K., Synthesis of Substituted Monohalobenzenes via Ortho-Selective Cross-Coupling of Dihalobenzenes with Electron-Donating Ortho-Directing Groups. Synthesis 2008, 2008 (19), 3180-3182.
- A. Widdowson, D.; Wilhelm, R., Palladium catalysed crosscoupling of (fluoroarene)tricarbonylchromium(0) complexes. *Chem. Commun.* 1999, (21), 2211-2212.
- Widdowson, D. A.; Wilhelm, R., Palladium catalysed Suzuki reactions of fluoroarenes. *Chem. Commun.* 2003, (5), 578-579.
- Yu, D.; Shen, Q.; Lu, L., Selective Palladium-Catalyzed C–F Activation/Carbon–Carbon Bond Formation of Polyfluoroaryl Oxazolines. J. Org. Chem. 2012, 77 (4), 1798-1804.
- Kim, Y. M.; Yu, S., Palladium(0)-Catalyzed Amination, Stille Coupling, and Suzuki Coupling of Electron-Deficient Aryl Fluorides. J. Am. Chem. Soc. 2003, 125 (7), 1696-1697.
- 23. Cargill, M. R.; Sandford, G.; Kilickiran, P.; Nelles, G., Pd-catalyzed sp2–sp cross-coupling reactions involving C–F bond activation in highly fluorinated nitrobenzene systems. *Tetrahedron* **2013**, *69* (2), 512-516.
- Luo, H.; Wu, G.; Xu, S.; Wang, K.; Wu, C.; Zhang, Y.; Wang, J., Palladium-catalyzed cross-coupling of aryl fluorides with Ntosylhydrazones via C–F bond activation. *Chem. Commun.* 2015, 51 (68), 13321-13323.
- He, J.; Yang, K.; Zhao, J.; Cao, S., LiHMDS-Promoted Palladium-Catalyzed Sonogashira Cross-Coupling of Aryl Fluorides with Terminal Alkynes. *Org. Lett.* 2019, 21 (23), 9714-9718.
- van der Veen, L. A.; Keeven, P. H.; Schoemaker, G. C.; Reek, J. N. H.; Kamer, P. C. J.; van Leeuwen, P. W. N. M.; Lutz, M.; Spek, A. L., Origin of the Bite Angle Effect on Rhodium Diphosphine Catalyzed Hydroformylation. *Organometallics* 2000, 19 (5), 872-883
- 27. van Leeuwen, P. W. N. M.; Kamer, P. C. J., Featuring Xantphos. *Catal. Sci. Technol.* **2017**, *8*, 26-113.
- Zhang, J.; Bellomo, A.; Creamer, A. D.; Dreher, S. D.; Walsh, P. J., Palladium-Catalyzed C(sp³)-H Arylation of Diarylmethanes at Room Temperature: Synthesis of Triarylmethanes via Deprotonative-Cross-Coupling Processes. *J. Am. Chem. Soc.* 2012, 134, 13765–13772.
- Zhang, J.; Bellomo, A.; Trongsiriwat, N.; Jia, T.; Carroll, P. J.;
 Dreher, S. D.; Tudge, M. T.; Yin, H.; Robinson, J. R.; Schelter, E. J.; Walsh, P. J., NiXantphos: A Deprotonatable Ligand for Room-Temperature Palladium-Catalyzed Cross-Couplings of Aryl Chlorides. J. Am. Chem. Soc. 2014, 136 (17), 6276-6287.
- Schoenebeck, F.; Houk, K. N., Ligand-Controlled Regioselectivity in Palladium-Catalyzed Cross Coupling Reactions. J. Am. Chem. Soc. 2010, 132 (8), 2496-2497.
- Senn, H. M.; Ziegler, T., Oxidative Addition of Aryl Halides to Palladium(0) Complexes: A Density-Functional Study Including Solvation. *Organometallics* 2004, 23 (12), 2980-2988.
- Kozuch, S.; Amatore, C.; Jutand, A.; Shaik, S., What Makes for a Good Catalytic Cycle? A Theoretical Study of the Role of an Anionic Palladium(0) Complex in the Cross-Coupling of an Aryl Halide with an Anionic Nucleophile. *Organometallics* 2005, 24 (10), 2319-2330.
- 33. Portnoy, M.; Milstein, D., Mechanism of aryl chloride oxidative addition to chelated palladium(0) complexes. *Organometallics* **1993**, *12* (5), 1665-1673.
- Zhang, J.; Sha, S.-C.; Bellomo, A.; Trongsiriwat, N.; Gao, F.; Tomson, N. C.; Walsh, P. J., Positional Selectivity in C-H Functionalizations of 2-Benzylfurans with Bimetallic Catalysts. *J. Am. Chem. Soc.* 2016, *138* (12), 4260-4266.

- Sha, S.-C.; Tcyrulnikov, S.; Li, M.; Fu, Y.; Kozlowski, M. C.; Walsh, P. J.; Hu, B., Cation-π Interactions in the Benzylic Arylation of Toluenes with Bi-metallic Catalysts. *J. Am. Chem. Soc.* 2018, *140*, 12415-12423.
- Jiang, H.; Sha, S.-C.; Jeong, S. A.; Manor, B. C.; Walsh, P. J., Ni(NIXANTPHOS)-Catalyzed Mono-Arylation of Toluenes with Aryl Chlorides and Bromides. *Org. Lett.* 2019, 21, 1735–1739.
- Yoshikai, N.; Nakamura, E., Mechanism of Substitution Reaction on sp2-Carbon Center with Lithium Organocuprate. *J. Am. Chem.* Soc. 2004, 126 (39), 12264-12265.
- Yamanaka, M.; Nakamura, E., Thermodynamic and Kinetic Control in Selective Ligand Transfer in Conjugate Addition of Mixed Organocuprate Me(X)CuLi. J. Am. Chem. Soc. 2005, 127 (13), 4697-4706.
- Yoshikai, N.; Matsuda, H.; Nakamura, E., Hydroxyphosphine Ligand for Nickel-Catalyzed Cross-Coupling through Nickel/Magnesium Bimetallic Cooperation. J. Am. Chem. Soc. 2009, 131 (27), 9590-9599.
- Yoshikai, N.; Mashima, H.; Nakamura, E., Nickel-Catalyzed Cross-Coupling Reaction of Aryl Fluorides and Chlorides with Grignard Reagents under Nickel/Magnesium Bimetallic Cooperation. J. Am. Chem. Soc. 2005, 127 (51), 17978-17979.
- 41. For an example involving Ni and Al cooperation see: Baird, D. A.; Jamal, S.; Johnson, S. A., Influence of the Transmetalating Agent in Difficult Coupling Reactions: Control in the Selectivity of C–F Bond Activation by Ni(0) Complexes in the Presence of AlMe3. Organometallics 2017, 36, 1436-1446.
- Knochel, P.; Dohle, W.; Gommermann, N.; Kneisel, F. F.; Kopp, F.; Korn, T.; Sapountzis, I.; Vu, V. A., Highly Functionalized Organomagnesium Reagents Prepared through Halogen-Metal Exchange. *Angew. Chem. Int. Ed.* 2003, 42 (36), 4302-4320.
- Li, G.; Szostak, M., Kinetically Controlled, Highly Chemoselective Acylation of Functionalized Grignard Reagents with Amides by N-C Cleavage. *Chem. Eur. J.* 2020, 26 (3), 611-615
- Adrio, J.; Carretero, J. C., Functionalized Grignard Reagents in Kumada Cross-Coupling Reactions. *ChemCatChem* 2010, 2 (11), 1384-1386.
- Martin, R.; Buchwald, S. L., Palladium-Catalyzed Suzuki-Miyaura Cross-Coupling Reactions Employing Dialkylbiaryl Phosphine Ligands. Acc. Chem. Res. 2008, 41 (11), 1461-1473
- 46. Amatore, C.; Pfluger, F., Mechanism of oxidative addition of palladium(0) with aromatic iodides in toluene, monitored at ultramicroelectrodes. *Organometallics* **1990**, *9* (8), 2276-2282.
- Yoshikai, N.; Matsuda, H.; Nakamura, E., Ligand Exchange as the First Irreversible Step in the Nickel-Catalyzed Cross-Coupling Reaction of Grignard Reagents. J. Am. Chem. Soc. 2008, 130 (46), 15258-15259.

- Martin, R.; Buchwald, S. L., Pd-Catalyzed Kumada-Corriu Cross-Coupling Reactions at Low Temperatures Allow the Use of Knochel-type Grignard Reagents. J. Am. Chem. Soc. 2007, 129 (13), 3844-3845.
- Martin, R.; Buchwald, S. L., Palladium-Catalyzed Suzuki-Miyaura Cross-Coupling Reactions Employing Dialkylbiaryl Phosphine Ligands. Acc. Chem. Res. 2008, 41, 1461-1473.
- Popp, B. V.; Thorman, J. L.; Morales, C. M.; Landis, C. R.; Stahl,
 S. S., "Inverse-Electron-Demand" Ligand Substitution: Experimental and Computational Insights into Olefin Exchange at Palladium(0). J. Am. Chem. Soc. 2004, 126 (45), 14832-14842.
- Álvarez, R.; Pérez, M.; Faza, O. N.; de Lera, A. R., Associative Transmetalation in the Stille Cross-Coupling Reaction to Form Dienes: Theoretical Insights into the Open Pathway. Organometallics 2008, 27 (14), 3378-3389.
- Ribagnac, P.; Blug, M.; Villa-Uribe, J.; Le Goff, X.-F.; Gosmini,
 C.; Mézailles, N., Room-Temperature Palladium-Catalyzed
 Negishi-Type Coupling: A Combined Experimental and
 Theoretical Study. Chem. Eur. J. 2011, 17 (51), 14389-14393.
- González-Pérez, A. B.; Álvarez, R.; Faza, O. N.; de Lera, Á. R.; Aurrecoechea, J. M., DFT-Based Insights into Pd–Zn Cooperative Effects in Oxidative Addition and Reductive Elimination Processes Relevant to Negishi Cross-Couplings. *Organometallics* 2012, 31 (5), 2053-2058.
- Groom, C. R.; Bruno, I. J.; Lightfoot, M. P.; Ward, S. C., The Cambridge Structural Database. Acta Cryst. 2016, 72, 171-179.
- Tang, Y.; Zakharov, L. N.; Rheingold, A. L.; Kemp, R. A., Synthesis and Structural Characterization of Magnesium Amide Complexes Containing -N[(R)(SiMe3)] Ligands. Organometallics 2005, 24 (5), 836-841.
- Kovbasyuk, L.; Hoppe, M.; Pritzkow, H.; Krämer, R., A Versatile Approach to the Intramolecular Organization of Two Bipyridine-Like Chelating Units in a Polytopic Ligand. *Eur. J. Inorg. Chem.* 2001, 2001 (5), 1353-1360.
- Zuniga, M. F.; Kreutzer, J.; Teng, W.; Ruhlandt-Senge, K., Lithium Aryloxo Magnesiates: an Examination of Ligand Size and Donor Effects. *Inorg. Chem.* 2007, 46 (24), 10400-10409.
- Pécharman, A.-F.; Hill, M. S.; McMullin, C. L.; Mahon, M. F., Magnesium Boryl Reactivity with 9-BBN and Ph3B: Rational B-B' Bond Formation and Diborane Isomerization. *Angew. Chem. Int. Ed.* 2017, 56 (51), 16363-16366.
- Garçon, M.; Bakewell, C.; Sackman, G. A.; White, A. J. P.; Cooper, R. I.; Edwards, A. J.; Crimmin, M. R., A hexagonal planar transition-metal complex. *Nature* 2019, 574, 390–393.

TOC image

